

Paths of Bacteriochlorophyll *c* Deexcitation in Green Photosynthetic Bacteria and in a Model System

A. Planner,¹ B. Susła,¹ M. Nowicki,¹ K. Klaczyńska,¹ and D. Frąckowiak^{1,2}

Received August 7, 1998; accepted December 1, 1998

Absorption, photoacoustic, and fluorescence spectra of green bacteria cells, their fragments, and artificial oligomers of bacteriochlorophyll *c*, with all samples embedded in polyvinyl alcohol films, were measured. The topography of polymer films without pigment and containing pigment oligomers or of monomers and small aggregates was established using atomic force microscopy. The images of these three types of films were different. The dimensions of oligomers were evaluated. On the basis of thermal deactivation of various pigment forms as well as on the grounds of previously measured lifetimes of their fluorescence, conclusions concerning excitation energy transfer between various pigment forms in organisms and in a model system were drawn.

KEY WORDS: Bacteriochlorophyll *c*; excitation energy transfer; pigment oligomers; polyvinyl alcohol film; thermal deactivation.

INTRODUCTION

Bacteriochlorophyll *c* in green photosynthetic bacteria occurs predominantly as oligomers located in chlorosomes, giant antenna complexes harvesting light for the process of photosynthesis [1]. Part of the pigment is present in organisms in a lower degree of aggregation or even in a monomeric state [2]. The red absorption band of oligomers is located at about 752 nm, whereas the band of the same transition for the monomeric state of pigment appears at about 670 nm. In the same region, about 670 nm, is located absorption of bacteriopheophytin *c* and also of some type of chlorophyll present at a low concentration [2].

The factor causing disaggregation of bacteriochlorophyll *c* (BChl *c*) causes a decrease in the 752-nm band and an increase in 670-nm absorption but the pigment orientation is largely preserved [3], which suggests that disaggregated pigment is still located inside of chlo-

rosomes. The same conclusion follows from reversible disaggregation and aggregation processes [4].

It is known that in native bacteria the energy harvested by chlorosomes is very efficiently transferred, through other pigment-protein complexes, to reaction centers and it is changed into the chemical energy necessary for hydrocarbon synthesis. The oligomers, with spectral properties very similar to natural, can be produced in model systems such as solutions, nematic liquid crystals, and polymer film [5–10]. Model aggregate structures were proposed on the basis of the ring-current effects on ¹H and ¹³C nuclei [9] and by analogy with other chlorophyll derivative aggregation [10].

In this work we investigate the dimensions of such artificial aggregates of BChl *c* in polymer film by studying the surface morphology of the film with and without pigment oligomers using atomic force microscopy. Such measurements also deliver information on the change in polymer topography due to the presence of pigment oligomers or monomers and small aggregates.

In order to investigate the paths of deexcitation of pigment in organisms and in the model system, we compare the thermal deactivation and emission of fluores-

¹ Institute of Physics, Poznań University of Technology, Piotrowo 3, 60-965 Poznań, Poland.

² To whom correspondence should be addressed.

cence of excited BChl *c* in organisms (bacteria cells or cell fragments) and in polymer polyvinyl alcohol (PVA) film. It was shown previously [6,7] that BChl *c*, in a model system as well as in bacteria, exhibits intensive delayed luminescence due to oligomer emission (about 750–800 nm) or to monomer emission (about 670 nm), depending on the state of pigment aggregation [5,6,11]. Both forms of pigment can take part in trapping part of the excitation and emitting it with an efficiency comparable to that of delayed emission, therefore we decided to concentrate on other possible paths of deexcitation: thermal deactivation (TD) and emission of fluorescence. These both paths of deexcitation are much more efficient than the emission of delayed luminescence.

MATERIALS AND METHODS

Samples

Prosthecochloris aestuarii (*Chloropseudomonas ethylica*), 2K strain, was grown anaerobically in a culture medium described by Holt [12] with 1400-lux illumination at 4°C. Whole bacteria or their fragments (obtained by sonification for 15 min at 4°C and centrifugation at 36,000g) were introduced into an aqueous solution of polyvinyl alcohol (PVA) mixed with resin (AG1-XB0) to obtain a nonacidic solvent (pH 7 to 7.4). The PVA films were produced and stretched as described previously [13,14]. Bchl *c* was obtained from the same organisms. The homologue (*E, E*)-BChl *c_f* [15] was extracted and purified as described previously [16]. The pigment was introduced into the same PVA solution with a resin mixture.

Spectral Measurements

Absorption spectra were measured with a Specord M40 Zeiss spectrophotometer. Fluorescence spectra were recorded with an arrangement constructed in our laboratory with an on-line computer and a Hamamatsu R928 photomultiplier as a receiver. All fluorescence spectra were corrected for the spectral sensitivity of the used system.

Photoacoustic spectra (PAS) were measured with a single-beam spectrometer built in our laboratory equipped with an MTEC Model 300 photoacoustic cell [17,18].

Atomic Force Microscopy

A room-temperature atomic force microscope (AFM) (OMICRON) was used to study the topography

[19,20] of polymers with and without pigment oligomers or monomers and small aggregates.

AFM images in the constant force mode were taken for all three samples in two regions. The measurements were made in air at 10°C. The sample was placed on a single-tube piezoelectric translator and tips of silicon nitride (Si₃N₄) fixed under the cantilever were used. The maximal area available to scan was 5000 × 5000 nm² and typical images consisted of 256 × 246 lines/points. The scan rate was within the range of a few hertz per line. The AFM resolution was 0.01 nm in the vertical direction and 0.05 nm in the surface plane. The lateral and vertical calibration was carried out by imaging the known atomic structure and height of the atomic steps of mica.

RESULTS AND DISCUSSION

As follows from the whole-bacteria absorption spectra (Fig. 1a), the content of disaggregated BChl *c* in such a sample is very low (a low 670-nm maximum with respect to the oligomer maximum at 752 nm). The thermal deactivation value, calculated as the ratio of the photoacoustic signal (PAS) (Fig. 1a) to the absorbed energy, is higher in the monomer absorption region (at 670nm) than in a region of oligomer absorption (at 750 nm) (Table I). This is an unexpected result because usually aggregated pigments convert their excitation into heat more efficiently than pigment in the monomeric forms. The lower fluorescence yield of oligomers than of monomers also follows from the much shorter lifetime of oligomer than of monomer emission [8]. In oligomer pigments in whole-bacteria cells, competition among emission of fluorescence, thermal deactivation of excitation, and transfer of excitation through the chain of the acceptors and donors to the reaction centers occurs. From Table I it follows that the monomers of BChl *c* have to be separated from this chain, whereas the oligomers are very efficient in transferring their excitation.

In the case of bacteria fragments (Fig. 1b) the monomeric pigment concentration is higher than in whole bacteria and BChl *c* is partially pheophytinized (as follows from the shape of the Soret band in Fig. 1b) This is a result of bacterial ultrasonic fragmentation [3]. For bacteria fragments the photoacoustic and absorption spectra have similar shapes (Fig. 1b). The calculated thermal deactivation (TD) values (Table I) are similar for both main maxima. The similar TD values observed for bacteria fragments of both pigments forms can occur in two cases: when the TD values of both forms, monomeric and oligomeric, are similar or with very quick and efficient

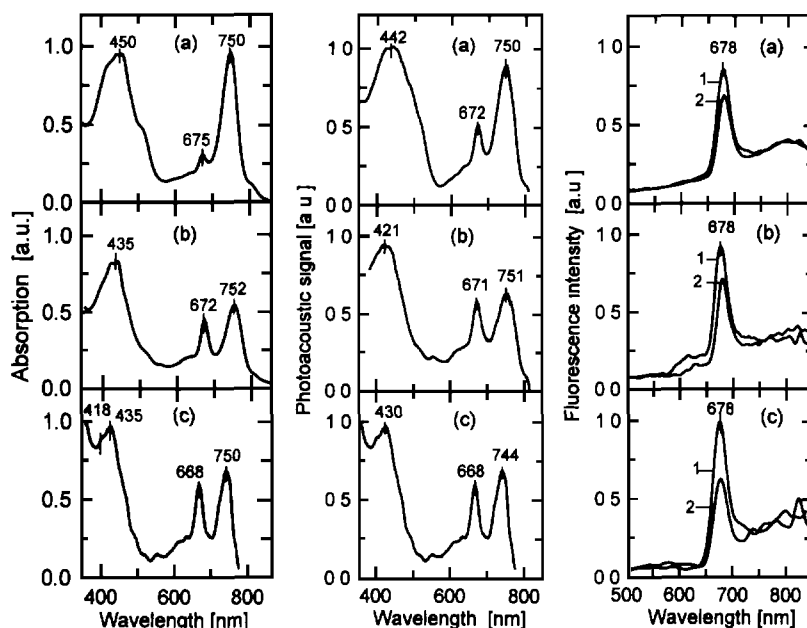


Fig. 1. Absorption, photoacoustic, and fluorescence spectra of samples embedded in PVA films (a) bacteria, (b) bacteria fragments, (c) and BChl *c* partially in the monomeric (absorption at 668 nm) and partially in the oligomeric state (absorption at 744–750 nm).

excitation energy transfer from monomers to oligomers followed by TD in oligomers. The first case is excluded by fluorescence lifetime measurements [8]. In bacteria fragments the oligomers are not the last acceptor of excitation because a TD value similar to that for the whole bacteria is observed (Table I). The low TD of monomers could be due to rather efficient excitation transfer from monomers to oligomers followed by the exchange of the excitation into heat in oligomers. But in such a case the monomer fluorescence should be quenched. From the present results it follows that at excitation in the region of monomer absorption in a Soret band, intensive emission at 680 nm is observed, whereas at excitation in the oligomer absorption range (at 450 nm), only very low long-wavelength emission appears (Figs. 1a and b). The contributions to absorption of each form in the regions of excitation used are comparable. It is possible that the excitation transfer from monomers to oligomers is very

quick in one pool of monomeric pigment, whereas the second pool is engaged in efficient fluorescence emission. It is known that several forms of pigments contribute to 670-nm emission, therefore the observed results can be explained by the existence of various pools of pigments with different efficiencies of excitation energy transfer. This is in agreement with our previous results [8,16]. One pool of pigment molecules could be engaged in efficient ET to oligomers, where energy is converted into heat and eventually transferred to the next steps in the energy transfer chain, whereas the second pool could be separated from the excitation energy chain and, as a result, is engaged predominantly in the emission of fluorescence exhibiting a low TD efficiency in monomers. The observed PAS spectra are the result of the superposition of contributions from all pigment forms.

Figure 1c presents the spectra of partially oligomerized Bchl *c* in PVA. Both absorption and PAS spectra exhibit maxima belonging to both forms of pigment. The TD of artificial oligomers is similar to that of monomers but both values are much higher than for TD of oligomers in bacteria (Table I). This is because oligomers in the model system are the final acceptors of excitation. It also shows that, in this case, excitation energy transfer from monomers to oligomers is efficient. The artificial oligomer emission is much stronger than oligomer emission in bacteria. A similar conclusion followed from analysis

Table I. Thermal Deactivation (TD) Calculated as the Ratio of the Photoacoustic Signal to the Absorbed Energy

| Sample | TD (670 nm) | TD (750 nm) |
|--|-------------|-------------|
| Whole bacteria | 0.029 | 0.014 |
| Bacteria fragments | 0.014 | 0.013 |
| Oligomers of BChl <i>c</i> in PVA film | 0.160 | 0.159 |

of the fluorescence decay of similar samples [8]. The oligomer fluorescence lifetimes values in the model sample and in bacteria are much shorter than the monomer decays. For artificial oligomers this is due only to the high TD yield, whereas for whole bacteria it is also related to excitation transfer to the next energy acceptor—bacteriochlorophyll *a*.

Figure 2 shows the spectra for a model sample with a low degree of pigment oligomerization, whereas Fig. 3 presents the same types of spectra for an almost completely oligomeric sample. In the first case (Fig. 2) the change in the wavelength of excitation changes the ratio of monomer (at 677 nm)-to-oligomer (at 787 nm) emission. In the second case (Fig. 3) at both wavelengths of excitations in a region of predominant monomer absorption (435 nm) as well as at excitation in oligomer absorption (at 450 nm), only oligomer emission is seen.

Both paths of deexcitation, fluorescence emission and TD, are much more efficient for the artificial oligomers than for oligomers in bacteria, therefore in bacteria there has to be some additional path of deexcitation competing with these two investigated paths. It was shown [19] that natural chlorosomal oligomers are not able to emit electrons under illumination by visible light. Therefore the energy is not used for antenna photoionization. All these facts strongly suggest that excitation is trans-

ferred from natural oligomers through other complexes [1] to reaction centers, where it is used for photoreaction. Immobilized bacteria are not in the natural situation but it seems that some photochemical reactions in reaction centers can occur and therefore part of the excitation is dissipated in this way. The rather high TD yield of artificial BChl *c* is in agreement with the very short time of fluorescence decay observed for such samples [8].

Several spectral properties of natural and artificial oligomers are similar. They exhibit absorption and fluorescence maxima in similar positions (Figs. 1–3). The dimensions of chlorosome rods are known, but it is possible that several oligomers of different structures [9,10] are combined to form every rod. To gather information on the dimensions of artificial oligomers, as well as on their mutual interaction with the polymer matrix, AFM images were taken. The images of three types of films are clearly different. The film with oligomers exhibits a structure that is much less regular and less pronounced than that of the film with monomers and small aggregates and is not seen in the film without pigment. The images taken at different locations of a given investigated film have quite similar characters.

It was not expected that pigment addition could modify the polymer film texture so greatly. It is possible that similar changes could occur for anisotropic matrixes used

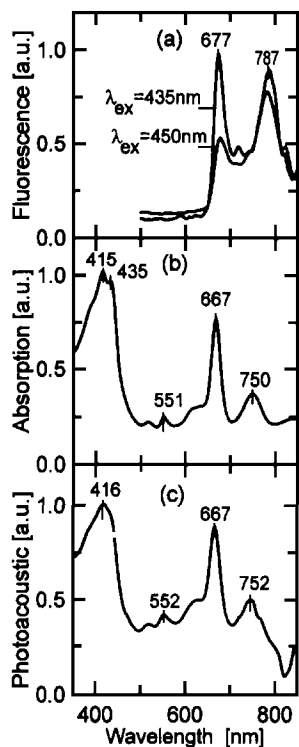


Fig. 2. Spectra of BChl *c* in PVA in a low degree of oligomerization.

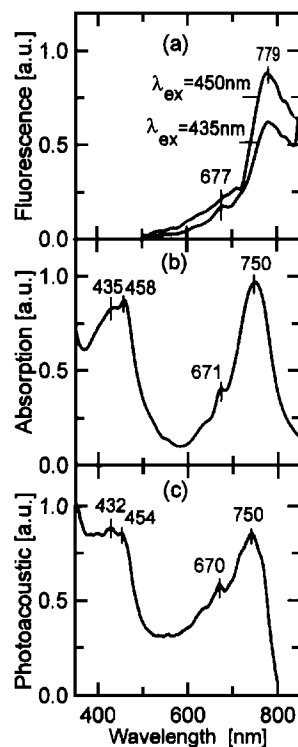


Fig. 3. BChl *c* in PVA film. Most of the pigment is in an oligomeric state.

for orientation of biological samples: bacteria, their fragments, and pigment-protein complexes [8]. From the comparison of the film with oligomers (spectra in Fig. 3) with the film with monomers and small aggregates (spectra in Fig. 2), it follows that the first film exhibits more regular elements that are better exposed in the vertical direction elements than the second film. The film without pigment exhibits not only regular but large "valleys" and "hills." On average the film without pigment is less flat than the pigmented samples. All films were prepared in an identical way. It is not clear if the oligomeric sample structure seen is due to such a large cluster of dye or if it is due to the change in polymer chain distribution which can surround the clusters of pigments forming larger structures. It is not excluded that hydrophobic pigment located near the hydrophilic film surface could also have some influence on the observed image. From the evaluation pigment contained in the unit of film volume and the comparison of this value with the volume of the observed structure, the second possibility seems more plausible. At any rate, the pigment clusters have to be smaller than the observed structure, therefore their diameters are not larger than 50 nm.

ACKNOWLEDGMENTS

This work was supported by Polish Committee for Scientific Research (KBN) Grant 6PO4AO1912 (1998) and by Poznań University of Technology Grant PB-62-153/98 BW.

REFERENCES

1. J. M. Olson (1998) *Photochem. Photobiol.* **67**, 61–75.
2. C. M. Otte, E. J. van de Meent, P. A. van Veelen, A. S. Pundsness, and J. Amesz (1993) *Photosynth. Res.* **35**, 159–169.
3. T. Martyński, D. Frąckowiak, J. Miyake, A. Dudkowiak, and A. Piechowiak (1998) *J. Photochem. Photobiol. B Biol.* **42**, 57–66.
4. K. Matsuura and J. M. Olson (1990) *Biochim. Biophys. Acta* **1019**, 233–238.
5. A. Dudkowiak, C. Francke, J. Amesz, A. Planner, I. Hanyż, and D. Frąckowiak (1996) *Spectrochim. Acta* **A52**, 251–264.
6. A. Dudkowiak, C. Francke, J. Amesz, A. Planner, and D. Frąckowiak (1996) *Spectrochim. Acta* **A52**, 1661–1669.
7. A. Planner, J. Goc, A. Dudkowiak, D. Frąckowiak, and J. Miyake (1997) *J. Photochem. Photobiol. B Biol.* **39**, 73–80.
8. D. Frąckowiak, A. Dudkowiak, A. Ptak, H. Malak, I. Gryczyński, and B. Zelent (1988) *J. Photochem. Photobiol. B Biol.* **44**, 231–239.
9. T. Mizoguchi, S. Sakamoto, Y. Koyama, K. Ogura, and F. Inagaki (1998) *Photochem. Photobiol.* **67**, 239–248.
10. T. Oba and H. Tamiaki (1998) *Photochem. Photobiol.* **67**, 295–303.
11. A. Dudkowiak, R. Cegielski, A. Ptak, A. Planner, E. Chrzumnicka, and I. Hanyż (1994) *Photosynthetica* **30**, 183–191.
12. C. Holt, S. F. Conti, and R. C. Fuller (1966) *J. Bacteriol.* **91**, 311–323.
13. D. Frąckowiak, S. Hotchandani, and R. M. Leblanc (1985) *Photochem. Photobiol.* **42**, 559–565.
14. D. Frąckowiak and A. Skibiński (1991) *Spectrosc. Lett* **24**, 1317–1328.
15. K. M. Smith (1994) *Photosynth. Res.* **41**, 23–26.
16. A. Dudkowiak, C. Francke, and J. Amesz (1995) *Photosynth. Res.* **46**, 427–433.
17. D. Ducharme, A. Tessier, and R. M. Leblanc (1979) *Rev. Sci. Instrum.* **50**, 42–43.
18. A. Resencwaig (1990) *Photoacoustic and Photoacoustic Spectroscopy*, Wiley Interscience, New York.
19. B. Susła (1997) in A. Rogalski, Y. Rutkowski, M. Majchrowski, and Y. Zieliński (Eds.), *Proceedings of SPIE*, Vol. 3179, p. 104.
20. B. Susła, R. Czajka, N. Sadowski, and T. Klimczuk (1997) *Physica C* **282–287**, 1503–1504.
21. A. Ptak, A. Dudkowiak, and D. Frąckowiak (1998) *J. Photochem. Photobiol. A Chem.* **115**, 63–68.